Proposed Modification to Increase Main Swept Back Wing Efficiency for Aircraft Aermacchi Siai S211

Naseer Abdul Razzaq Mousa
Assistant Lecturer
Engineering Affaire Department - University of Baghdad
E-mail:nasseer64@gmail.com

ABSTRACT

A winglet is devices attached at the wing tips, used to improve aircraft wing efficiency by reduction influence wing tips vortices and induct drag, increasing lift force at the wing tips and effective aspect ratio without adding greatly to the structural stress and weight in the wing structure. This paper is presented three-dimensional numerical analysis to proposed modification swept back wing by adding Raked winglets devices at the main wing tips belong the two seat trainer aircraft type Aermacchi Siai S211 by using Fluent ANSYS 13 software. CFD numerical analysis process was performed at the same flight boundary conditions indifferent wing angle of attacks with constant air flow velocity V_∞ =50 (m/sec), ambient pressure P_o=101325 (Pa), ambient temperature T_o=288.14 (K), and at air density ρ_o=1.225 (kg\m3) to both proposed wing model and the main aircraft wing model. The results are shown an improvement in aerodynamic parameters including increment lift coefficient to (0.22%-5.95%), reduction drag coefficient to (0.34% - 3.60%), increment wing load efficiency ratio to (2.62% - 7.30%), reduction induct drag coefficient C_{Di} to (7.65% - 13.11%) compared with the main aircraft wing model and achieved an improvement in aircraft flight maneuver abilities and stability controls especially during descent, approach, landing and takeoff with lower speed with shortage runway.

Key word: aerodynamics, theory of wing section, winglets, Aermacchi Siai s211 Aircraft.

التعديل المقترح لزيادة كفاءة الجناح المتراجع الى الخلف لطائرة Aermacchi Siai S211

نصير عبدالرزاق موسى
مدرس مساعد
قسم الشؤون الهندسية ـ جامعة بغداد

الخلاصة

الجنيحات الطرفية عبارة عن اجهزة تركب على اطراف الاجنحة تستخدم لتحسين كفاءة جناح الطائرة عن طريق تقليل تاثير الدوامات الهوائية الطرفية، وتاثير الكبح الحثي، زيادة قوة الرفع عند طرفي الجناح التي تؤدي الى زيادة تاثير نسبة باع الجناح الى المساحة الكلية بدون اضافة احمال واجهادات اضافية كبيرة لهيكل الجناح. يقدم هذا البحث التحليل العددي ثلاثي الابعاد لتعديلات مقترحة لجناح متراجع الى الخلف باضافة جنيحات طرفية مسلوبة الى الخلف الى الجناح الاساسي لطائرة تدريب ثنائية المقعد طراز (Aermacchi Siai S211) باستخدام البرنامج التحليلي (ANSYS 13.). تم تنفيذ عملية التحليل العددي لكلا الجناح المقترح والجناح الاساسي للطائرة في نفس ظروف الطيران المحددة لمختلف زوايا هجوم الجناح مع بثبوت سرعة جريان الهواء (V_∞ = 50 (m/sec), الضغط الجوي (P_o=101323 (Pa) ودرجة حرارة (T_o=288.14 (K) و كثافة الهواء (ρ_o=1.225 (kg\m3). اظهرت نتائج التحليل العددي تحسن في البارامترات الايروديناميكية لنموذج الجناح المقترح التي تتضمن زيادة معامل قوة الرفع معامل الرفع الى (0.22% - 5.95%), وتقليل معامل قوة الكبح الى (0.34% - 3.72%), وزيادة نسبة كفاءة الجناح الى (2.62% - 7.30%) , وتقليل معامل الكبح الحثي الى (7.65% - 17.37%)

بالمقارنة مع الجناح االاساسي للطائرة وحققت تحسن في قابلية الطائرة للمناورة واستقرارية السيطرة خصوصا اثناء النزول،والتقرب،والهبوط والاقلاع في سرعات طيران اقل في مسافة مدرج اقصر.

1. INTRODUCTION

The wings are the most important part to produce lift force of the aircraft. Wings vary in design depending upon the aircraft type and its purpose, **Abbott**, and **Doenhoff, 1959**. Induced drag is caused by the wingtip vortex, an unavoidable collateral effect of lift generation in a finite wing. It has been proven that modifications in the wingtip or the use of wingtip devices can minimize the induced drag expressively**, Cosin** and **Catalano, 2010**. Wingtip devices are usually increase the effective aspect ratio of a wing, with less added wingspan and intended to improve the efficiency of fixed-wing aircraft**, Abbott**, and **Doenhoff, 1959**. The wingtip devices increase the lift generated at the wing tip, and reduce the lift-induced drag caused by wingtip vortices, improving lift-to-drag ratio L / D. This increases fuel efficiency in powered aircraft, and cross-country speed in gliders, in both cases increasing range, The winglet converts some of the otherwise wasted energy in the wing tip vortex to an apparent thrust. This small contribution can be very worthwhile, provided the benefit offsets the cost of installing and maintaining the winglets during the aircraft's lifetime. Another potential benefit of winglets is that they reduce the strength of wing tip vortices, which trail behind the plane. When other aircraft pass through these vortices, the turbulent air can cause loss of control, possibly resulting in an accident, **Inam, et al,. 2010**.

2. RELATED WORKS

There are several works on "Aerodynamic characteristics of the winglet devices" were developed. **Cosin** and **Catalano, 2010**, performed aerodynamics analysis of the multi-winglets for low speed aircraft, baseline and six other different multiwinglets configurations were tested. The device led to 32% improvement in the Oswald efficiency factor, representing an increase of 7% in the maximum aerodynamic efficiency. Improvements of 12% in the maximum rate of climb and 7% in the maximum range were also obtained. **Azlin, et al., 2011**, a three-dimensional CFD analysis that was performed on a winglets rectangular wing of NACA$65_3$218 cross sectional airfoil. He was obtained that a comparison of aerodynamics characteristics of lift coefficient CL, drag coefficient CD and lift to drag ratio, L/D was made and it was found that the addition of the elliptical and semi circular winglet gave a larger lift curve slope and higher Lift-to-Drag Ratio in comparison to the baseline wing alone. **Smith** and **Komerath, 2001**, examined the potential of multi-winglets for the reduction of induced drag without increasing the span of aircraft wings. Wind tunnel models were constructed using a NACA 0012 airfoil section for the untwisted, rectangular wing and flat plates for the winglets. Testing of the configurations occurred over a range of Reynolds numbers from 161,000 to 300,000. The results show that certain multi-winglet configurations reduced the wing induced drag and improved L/D by 15-30% compared with the baseline 0012 wing. **Hossain, et al., 2012**, studied the aerodynamic characteristic for aircraft wing model with and without bird feather like winglet. The aerofoil used to construct the whole structure is NACA 65_3-218 Rectangular wing and this aerofoil has been used to compare the result with previous research using winglet. The experimental result shows 25-30 % reduction in drag coefficient and 10-20 % increase in lift coefficient by using bird feather like winglet at angle of attack of 8 degree.

3. WINGTIP VORTICES

Wingtip vortices are circular patterns of rotating air left behind a wing. Vortices form because of the difference in pressure between the upper and lower surfaces of a wing that is

operating at a positive lift, air flows from the lower surface out around the tip to the upper surface of the wing in a circular fashion caused to pressure on the upper and lower surface become equal at the wing tips **Fig. 1**. The spanwise flow on the finite wing is meet at the trailing edge, they give rise to a swirling motion that, within a short distance downstream, is concentrated into the two well-known tip vortices **Fig. 2**. This process can be idealized as a "horseshoe" vortex system **Fig. 3**. The wingtip vortices contain a large amount of translational and rotational kinetic energy which is produce a stream of air downward after the wing called downwash or induct velocity (*wi*) which is directly responsible for the appearance of one of the components of resistance aerodynamic, induced drag (*Di*), reduce the wing effective angle of attack and increase aircraft engine fuel conception ratio, **Thomas, 1999**.

4. WINGLETS

Wingtip devices are usually intended to improve the efficiency of the fixed-wing aircraft by partial recovery of the tip vortex energy, increase effective aspect ratio without increasing wing span, increase the lift generated at the wingtip by smoothing the airflow across the upper wing near the tip, reduce the lift-induced drag caused by wingtip vortices and increase aircraft power plant efficiency **Faye, et al., 2007**. There are many types of winglets which applicant in aircrafts such as transporting, cargo, VIP transporting aircrafts. Winglets can be classified depending of the winglet part attachment with main wingtips, so commonly they are three types wing with fence winglets, wing with blended winglets and wing with Raked winglets see **Figs. 4a, 4b,** and **4c**.

5. AERODYNAMICS BACKGROUND

Usually flight operation consist of take-off, climb, cruise, turn, maneuver, descent, approach and landing, so the wing must produce sufficient lift force while the drag force must be minimum.

The lift force can be written as:

$$L= 1/2\ \rho\ V_{\infty}^2\ S\ C_L \quad (1)$$

The drag force can be written as:

$$D=1/2\ \rho\ V_{\infty}^2\ S\ C_D \quad (2)$$

Where:

ρ - air flow density. (Kg/m^3)

V_{∞} - air flow velocity. (m/sec)

S - wing area. (m^2)

C_L - wing lift coefficient (dimensionless)

C_D - wing drag coefficient (dimensionless)

Induced drag is caused by the wingtip vortex in finite wing and can be written as, **Anderson, 2005**.

$$D_i=\frac{2L^2}{\rho\pi b^2 V_{\infty}^2 e} \quad (3)$$

Where:
L is the lift, ρ fluid density, b is wingspan, V velocity and e is efficiency factor, in general e<1 and depends on the wing shap.
Induct drag coefficient is

$$C_{di} = \frac{{C_L}^2}{\pi e AR} \quad (4)$$

Where:
The induced drag coefficient C_{di} is equal to the square of the lift coefficient C_L divided by the quantity: π (3.14159) times, wing efficiency factor time's (e) the aspect ratio AR,

$$AR = \frac{b^2}{S} \quad (5)$$

For a wing, the total drag coefficient, C_D is equal to the parasite drag coefficient at zero lift C_{do} plus the induced drag coefficient C_{di}.

$$C_D = C_{do} + C_{di} \quad (6)$$

Where parasite drag is C_{do} is skin friction drag due frictional shear stress integrated over the wing surface and pressure drag due to flow separation.
Induct angle of attack can be written as

$$\alpha_i = \frac{C_L}{\pi AR} \quad (7)$$

Effective angle of attack of the wing is:

$$\alpha_{eff} = \alpha - \alpha_i \quad (8)$$

Downwash velocity at the wing tip is:

$$w_i = -\frac{\Gamma_0}{2b} \quad (9)$$

Where Γ_0 is the circulation at the wing

$$\Gamma_0 = \frac{2V\infty \, S \, C_L}{b\pi} \quad (10)$$

7. CASE STUDY

Two seats trainer aircraft type Siai - Aermacchi S.211, **Figs. 5** and **6**, are analyzed in order to produce a new modification to improve the efficiency of the aircraft wing.
The main general technical data and characteristics of the aircraft are: **FAA, 2012**.

- Crew: two: student and instructor
- Length: 30 ft 6½ in, (9.31 m)
- Wingspan: 27 ft 8 in, (8.43 m)
- Height: 12 ft 5½ in, (3.8 m)

- Wing area: 135.63 ft², (12.6 m^2)
- Empty weight: 4,070 lb, (1.850 kg)
- Maximum takeoff weight: 6,050 lb, (2750 kg)
- Power plant: 1 × Pratt & Whitney JT15D-4C turbofan engine, 2,500 lb, (11.12 kN)

Aircraft performance: (Cruise altitude (25000 ft), 7620 m)
- Never exceed speed: Mach 0.8, (740 km/h, 400knots, 460 mph)
- Maximum speed: 360 knots, (667 km/h)
- Stall speed: 74 knots, (138 km/h)
- Range: 900 nm, (1,668 km, 1,036 miles)
- Service ceiling: 40,000 ft, (12,200 m)
- Rate of climb: 4,200 ft/min, (21 m/s)
- Thrust/weight: 0.413:1
- Acceleration limits: +6.0g (+58.9 m/s²)/-3.0g (-29.0 m/s²)

Aircraft wing geometry model, **Fig. 7**:
- Aspect Ratio AR is 5.52
- Wing root chord length C_r is 2 m,
- Wing tip chord C_t is 1 m.
- Taper ratio λ is 0.5
- Leading edge swept angle Λ_{LE} is 19^o
- Quarter chord swept angle $\Lambda_{1/4}$ is15^o
- Not twisted.
- No dihedral angle.
- Wing span b is 8.34 m
- Wing root cross section is airfoil Naca 64_2-215
- Wing tip cross section is airfoil Naca 64_2-212

The cross section airfoil Naca 64_2-215 and Naca 64_2-212 was selected as follow: **Sadraey, 2013**.

$$C_{L\ Vmax\ aircraft} = \frac{2xWxg}{\rho 7620 x Vmax^2 x\ S}$$

$$C_{L\ Vmax\ aircraft} = \frac{2x2750x9.81}{0.5502x185.27^2x12.6} = 0.2267$$

$C_{L\ Vmax\ wing}$ = 0.2267/0.95 = 0.23867

$C_{li\ airfoil}$ = 0.23867/0.9 = 0.26519

$C_{l\ ideal\ airfoil} \approx 0.2 \times 10 = 2$

$$C_{Lmax\ aircraft} = \frac{2xWxg}{\rho_o x Vstall^2 xS}$$

$C_{Lmax\ aircraft} = \frac{2x2750x9.81}{1.225x38.33^2x12.6} = 2.37$

$C_{Lmax\ wing}$ = 2.37/0.95 = 2.49 with flaps and slats down

$C_{lmax\ airfoil}$ = 2.49/0.9 = 2.76 with flaps and slats down

Proposed aircraft wing model is the aircraft main wing geometry with attached raked winglet bended up to 30^o, **Fig. 8**, where raked winglet tip is a small wing attached at the main wing tips and consist of selected Naca 64_2-212, Naca 64-012 and Naca 64-010 as a winglet cross section airfoils, **Fig. 9.** General characteristics of the proposed modification aircraft wing with raked winglet **Figs. 10**, **11** and **12** are:

- Main wing root chord Length C_r is 2 m.
- Main wing tip chord length C_t is 1 m.
- Winglet root chord length is 1 m.
- Winglet tip chord length is 0.3 m.
- Winglet area is 0.5 m^2.
- Winglet span is 0.67 m.
- Winglet bended up at the tip by 30^o.
- Winglet swept angle leading edge is 51^o.
- Winglet root cross section airfoil Naca 64_2-212
- Winglet intermediate cross section airfoil Naca 64-012
- Winglet tip cross section airfoil Naca 64-010
- Wing span b is 9.34 m
- Wing area is S is 13 m^2
- Taper ratio λ = 0.5 without winglets
- Aspect ratio AR= 6.71
- Leading edge swept angle Λ_{LE} = 19^o
- Quarter chord swept angle $\Lambda_{1/4}$ =15^o

8. MATHMATICAL MODEL

FLEUNT solves the Navier-Stokes equation which is includes expressions for the conservation of mass, momentum, pressure, species and turbulence, because the flow conditions are incompressible flow, the results are written as a continuity equation Eqs. (11) and (12) and Navier-Stokes equations for a viscous flow Eqs. (13a, 13b and 13c). **Anderson, 2005**. and **Fluent, 2005**.

$$\frac{\partial \rho}{\partial t} + \nabla.(\rho V) = 0 \qquad (11)$$

Where, ρ is fluid density, t is time, and V is the flow velocity vector field. If density (ρ) is a constant, as in the case of incompressible flow, the mass continuity equation.
Simplifies to a volume continuity equation:-

$$\nabla.(\rho V) = 0 \quad (12)$$

$$\frac{\partial(\rho u)}{\partial t} + \nabla.(\rho u V) = -\frac{\partial p}{\partial x} + \rho f x + (Fx)viscous \quad (13a)$$

$$\frac{\partial(\rho v)}{\partial t} + \nabla.(\rho v V) = -\frac{\partial p}{\partial y} + \rho f y + (Fy)viscous \quad (13b)$$

$$\frac{\partial(\rho w)}{\partial t} + \nabla.(\rho w V) = -\frac{\partial p}{\partial z} + \rho f z + (Fz)viscous \quad (13c)$$

The Momentum Eq. (14a, 14b, and 14c) for an inviscid flow are called the Euler equations.

$$\nabla.(\rho u V) = -\frac{\partial p}{\partial x} \quad (14a)$$

$$\nabla.(\rho u V) = -\frac{\partial p}{\partial x} \quad (14b)$$

$$\nabla.(\rho u V) = -\frac{\partial p}{\partial x} \quad (14c)$$

9. NUMERICAL ANALYSIS

The CFD numerical analysis is consisting of three stages as shown in **Fig. 13**. The pre-processing stage is include re-design Three-Dimensional model to the main wing without winglet and proposed wing with raked winglet, meshing models and flow control volume into the elements using GAMBIT 2.4.6. In addition, to ensure that the mesh created is sufficient to accurately model the flow behavior around the wing at air velocity with various angle of attacks at the straight flight, a grid independence study was conducted, **Fig. 14**. The second stage is the CFD numerical analysis process is solved to determine the grid check, definition boundary conditions, definition simulation flight parameters at various angle of attacks α =(0^o, 2^o, 4^o, 6^o, 8^o, 10^o, 12^o, 14^o, 16^o), flow air velocity $V\infty$ = 50 m / sec, ambient pressure 101325 pa, ambient temperature 288.14 K, dynamic viscosity 1.7894e-05 kg\m-s, air density 1.225 kg\m3 and ratio of specific heats is 1.4 (α), graphics simulations **Fig. 15**, **Fig. 16, Fig. 17**, and **Fig. 18.** Finally is the post-processing stage where the aerodynamics characteristics of the proposed wing with winglet model were found.

10. RESULTS AND DISCUSSIONS.

CFD numerical analysis results are discussed and focused on the proposed wing model improvements compared with the main wing model as follow:

- Improvement in the aerodynamic performance as a result of reduction influence wing tip vortices on the main wing, where **Table 1** represents magnitudes of lift coefficient C_L at different angle of attacks α, and **Fig. 19** represents graphics change of the lift coefficient C_L with constant air velocity at different angle of attacks.
- Reduction total drag coefficients of the wing as a result of effective winglet tip by reduction induct drag magnitude, where **Table 2** represents magnitude drag coefficient C_D at different angle of attacks α, **Fig. 20** represents graphics change of the drag coefficient C_D.

- Improvement in the aerodynamic wing efficiency by increasing magnitude of the wing efficiency C_L/C_D ratio as a result of effect winglet tip, where **Table 3** represents Lift-to-Drag coefficient ratio C_L/C_D, **Fig. 21** represents lift- to- drag coefficient ratio C_L/C_D graphics.
- The aerodynamic wing efficiency improved by decreasing magnitude of the C_D/C_L ratio as a result of influence decrease the wing drag coefficient and increases the wing lift coefficient, where **Table 4** represents drag-to lift coefficient ratio C_D/C_L, **Fig. 22** represents drag-to lift coefficient ratio C_D/C_F graphics.
- The aerodynamic wing efficiency improved by decreasing induct drag coefficient (C_{Di}) as a results of reduction influence of the wing tip vortices, where **Table 5** represents induct drag coefficient, **Fig. 23** represents induct drag coefficient graphics.
- Improvement in the aerodynamic lift force parameter of the wing as a result of increasing lift force at the wing tips by reduction influence magnitude wing tip vortices, where **Table 6** represents aerodynamic lift force, **Fig. 24** represents aerodynamic lift force graphics.
- The aerodynamic characteristics wing efficiency improved by decreasing magnitude of the wing tip vortices, where **Table 7** represents aerodynamic drag force, **Fig. 25** represents aerodynamic drag force graphics.
- Improvement in aerodynamic wing efficiency by decreasing magnitude of the induct angle of attack (α_i) and increase effective angle of attack (α_{eff}), where **Table 8** represents Induct Angle of Attack (α_i) and effective angle of attack (α_{eff}).

11. CONCLUSSION

Proposed modification on the main swept back wing is achieved an improvement in aircraft flight maneuver abilities and stability controls especially during descent, approach, landing and takeoff with lower speed with shortage runway by increasing the lift generated at the wingtip, effective angle of attack and lift-to-drag ratio as a result of smoothing the airflow across the upper wing near the tip and reduce the lift-induced drag caused by wingtip vortices, where **Table 9** represents the percentage gain of the aerodynamic parameters of the proposed wing as follow:

- Improved increment (0.22%-5.95%) to lift coefficient C_L and that lead to increasing lifting load on the wing especially during descent, approach, landing and takeoff with lower speed.
- Improved reduction (0.34% - 3.60%) in drag Coefficient C_D and that led to reduction engine power during cruise speed, reduction fuel consumption and reduce stall speed and takeoff – landing runway distance.
- Improved aircraft maneuver by increment wing load efficiency C_L/C_D to (2.62% - 7.30%).
- Improved reduction (7.65% - 13.11%) in induct drag coefficient as a result of influence winglet type by decreasing wing tip vortices, downwash velocity, especially during takeoff and landing operations.

REFERENCES

- Abbott, I. H., and von Doenhoff, A. E, 1959, *Theory of Wing Sections*, Dover, New York, 1959.
- Cosin, R. , Catalano, F.M. , Correa, L.G.N. , Entz, R.M.U. 2010, *Aerodynamic Analysis of Multi-Winglets for Low Speed Aircraft*, 27th International Congress of the Aeronautical Sciences.
- Mohammad Ilias Inam, Mohammad Mashud, Abdullah-Al-Nahian, S. M. S. Selim, 2010, *Induced Drag Reduction for Modern Aircraft without Increasing the Span of the Wing by Using Winglet*, International Journal of Mechanical & Mechatronics. IJMME-IJENS Vol: 10 No: 03,2010
- M. A Azlin, C.F Mat Taib, S. Kasolang and F.H Muhammad, 2011, *CFD Analysis of Winglets at Low Subsonic Flow*, Proceedings of the World Congress on Engineering 2011 Vol I WCE 2011, July 6 - 8, 2011, London, U.K.
- M. J. Smith•, N. Komerath, R. Ames, O. Wong, 2001, *Performance Analysis of a Wing with Multiple Winglets*, AIAA-2001-2407.
- Altab Hossain, Ataur Rahman, A.K.M. P. Iqbal, M. Ariffin, and M. Mazian, 2012, *Drag Analysis of an Aircraft Wing Model with and without Bird Feather like Winglet*, International Journal of Aerospace and Mechanical Engineering 6:1 2012.
- Thomas.F., 1999, *Fundamentals of Sailplane Design*, Translated by Judah Milgram, College Park Press, MD.
- Faye, R.; Laprete, R.; Winter, M. 2007, *Aero*, No. 17., *Boeing. Assessment of Wingtip Modifications to Increase the Fuel Efficiency of Air Force Aircraft*, National Academies Press, p.33
- D. Anderson, Jr. 2005, *Fundamentals of Aerodynamics*, Fourth Edition.
- FAA,2012, *Air - 320 Airworthiness Certification Branch Federal Aviation Administration*, Washington DC, September 28, 2012
- Mohammad Sadraey,2013, *Chapter 5 Wing Design*, Daniel Webster College, July 27, 2013
- Fluent, Inc. 2005, *Fluent 6.2*, User's Guide.

NOMENCLATURE

L : wing lift force (KN)
D : wing drag force (KN)
D_i : wing induct drag (KN)
C_L : wing lift coefficient (dimensionless)
C_D : wing drag coefficient (dimensionless)
C_{Di} : wing induct drag coefficient (dimensionless)
C_{do} : base drag coefficient at zero lift (dimensionless)
AR : wing aspect ratio(dimensionless)
b : wing span (m)
e : span efficiency factor < = 1
S : wing area (m^2)
A : wing angle of attack (Degree)
α_i : wing induct angle of attack (Degree)
α_{eff} : wing effective angle of attack (Degree)
w : wing downwash velocity at the wing tip (m/sec)
Γ_0 : wing circulation flow (rad/sec)
V_∞ : air flow velocity (m/sec)
C_r : wing cross section airfoil root chord length (m)
C_t : wing cross section airfoil tip chord length (m)
Λ : wing taper ratio (dimensionless)
Λ_{LE}: wing leading edge swept back angle. (Degree)
$\Lambda_{1/4}$: wing quarter chord swept back angle (Degree)

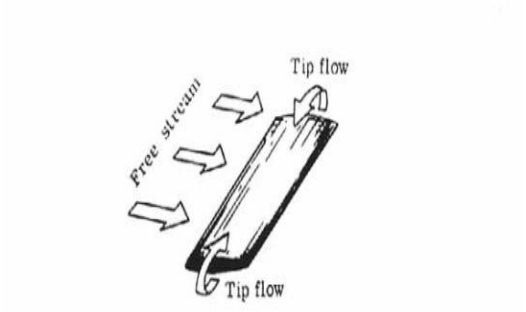

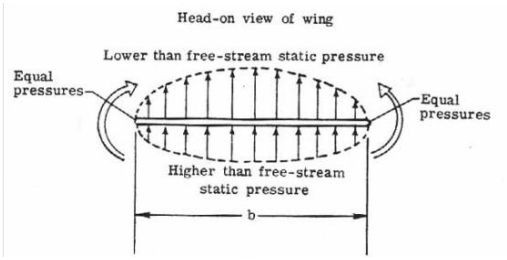

Figure 1. Static pressure distribution around the wing.

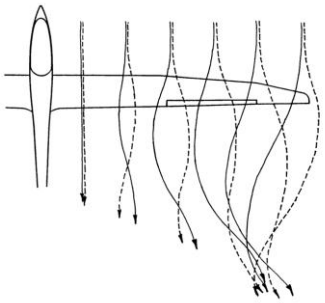

Figure 2. Spanwise flow on a finite wing - solid lines, upper surface; dashed lines, lower .

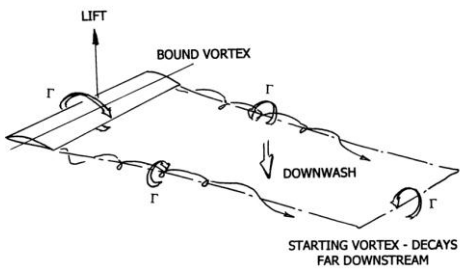

Figure 3. Idealized "horseshoe" vortex system.

Figure 4a. Wing with Fence Winglets.

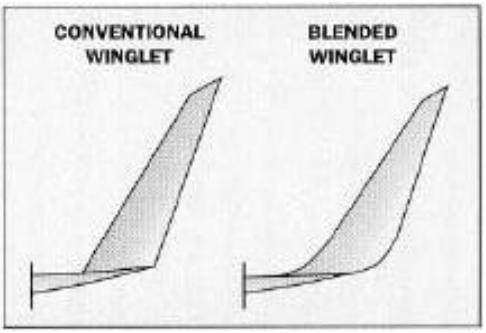

Figure 4b. Wing with blended winglets.

Figure 4c. Wing with raked winglets.

Figure 4. Winglets types.

Figure 5. Two seats trainer aircraft Siai-Aermacchi S211.

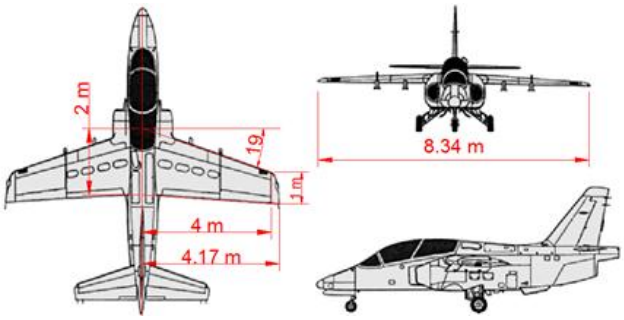

Figure 6. Aircraft dimensions.

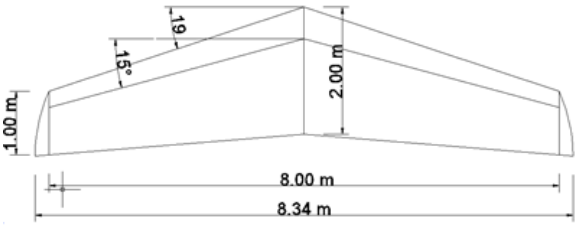

Figure 7. Aircraft wing geometry.

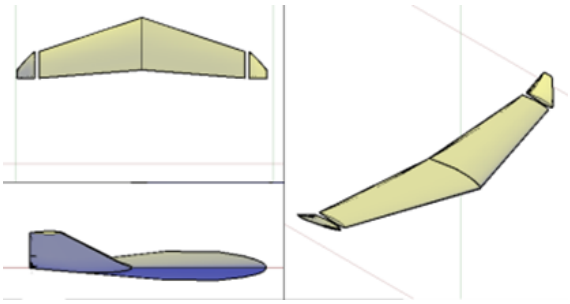

Figure 8. Proposed aircraft wing model .

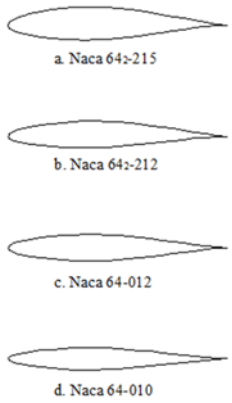

a. Main wing root airfoil type

b. Main wing tip airfoil type

c. Winglet root airfoil type

d. Winglet tip airfoil type

Figure 9. Wing cross section airfoil types.

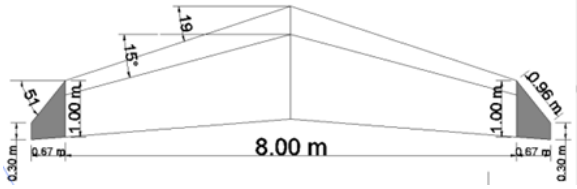

Figure 10. Proposed winglet tips dimensions

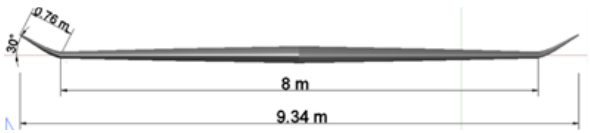

Figure 11. Front view proposed wing with raked winglet tips.

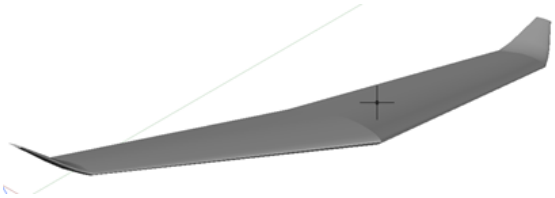

Figure 12. Modification wing model with raked winglets.

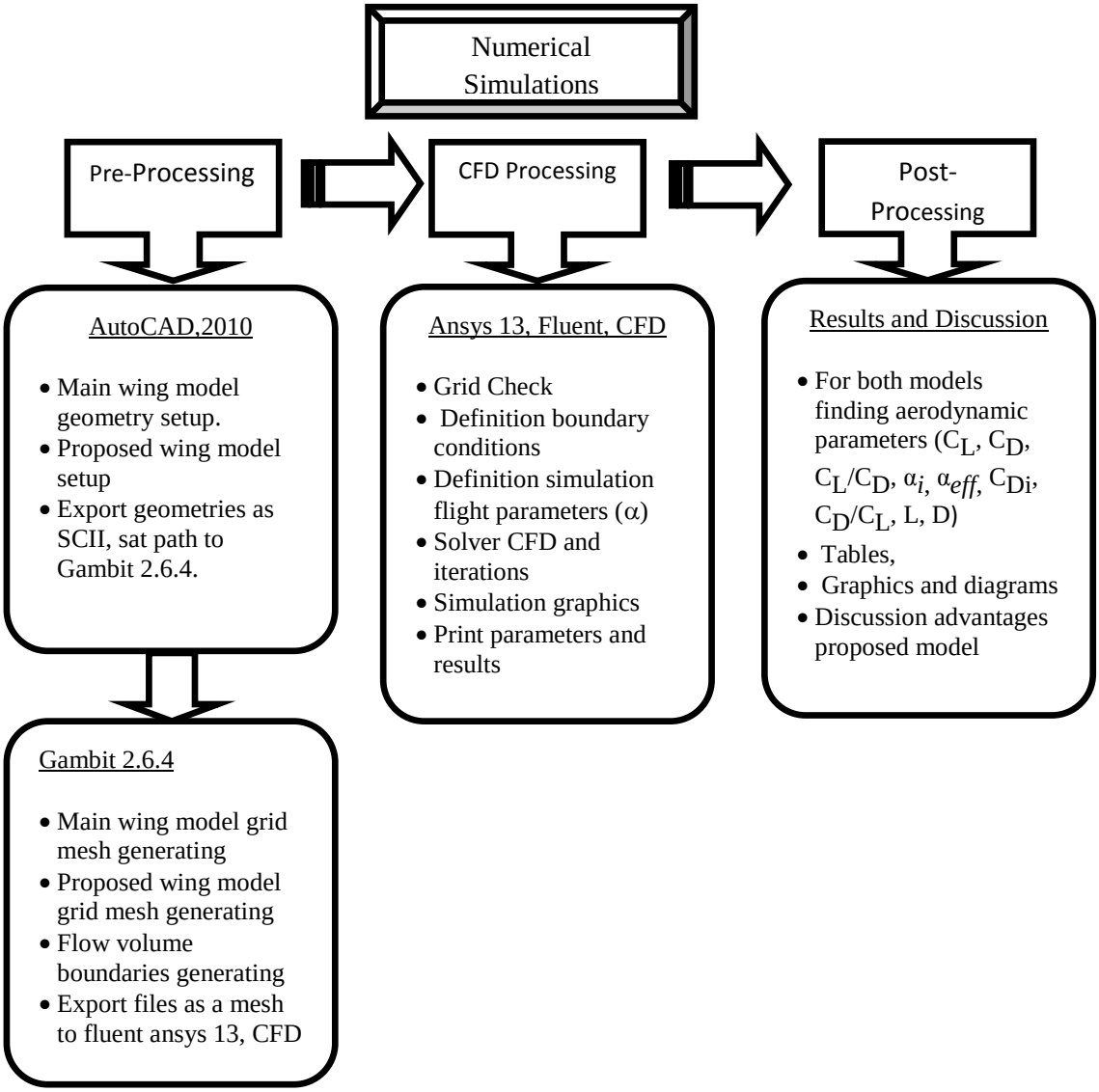

Figure 13. Numerical analysis simulation stages.

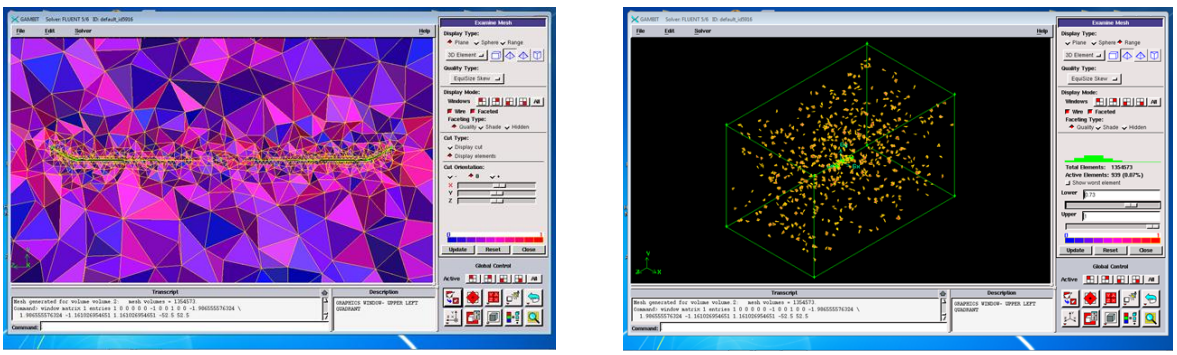

Figure 14. Grid mesh quality level of the proposed wing model.

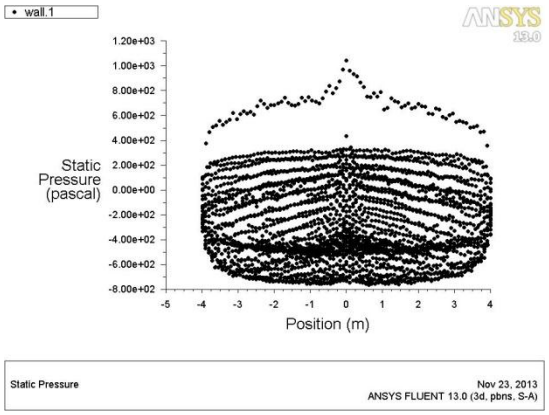

Figure 15. Static pressure distribution along span main wing model at $\alpha=0^{o}$.

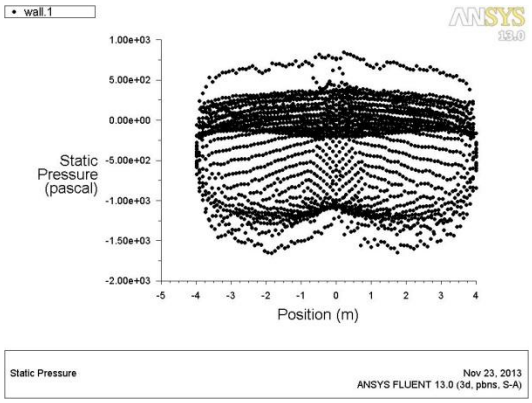

Figure 16. Static pressure distribution along span main wing model at $\alpha=6^{o}$.

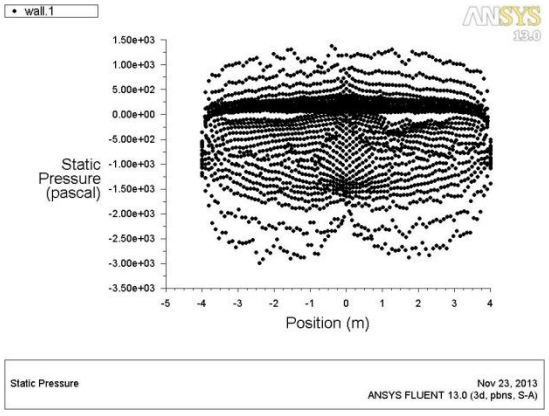

Figure 17. Static pressure distribution along span main wing model at $\alpha=12^{o}$.

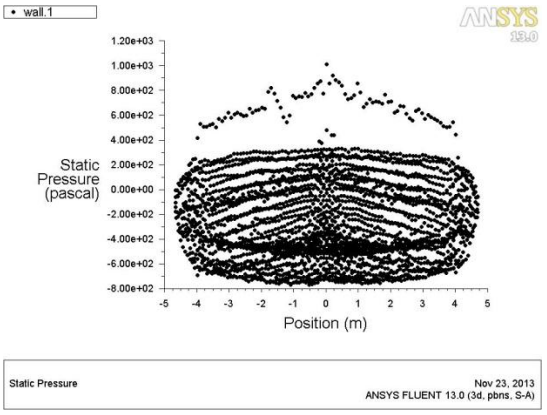

Figure 18. Static pressure distribution along span proposed wing model at $\alpha=0^{o}$

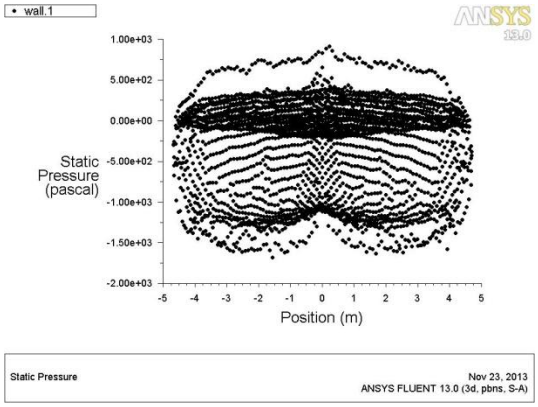

Figure 18. Static pressure distribution along span proposed wing model at $\alpha=6^{o}$.

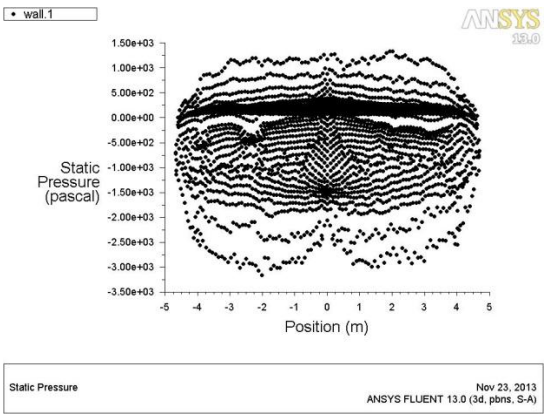

Figure 18. Static pressure distribution along span proposed wing model at $\alpha=12^{o}$.

Table 1. Lift coefficient C_L vs α.

Air Velocity V∞ (m/s)	α	CL Proposed Wing	CL Main Wing
50	0	0.117023	0.113869
	2	0.276141	0.26273
	4	0.428717	0.404643
	6	0.572105	0.546597
	8	0.702571	0.664326
	10	0.813211	0.778107
	12	0.902425	0.865405
	14	0.940456	0.919837
	16	0.929477	0.927423

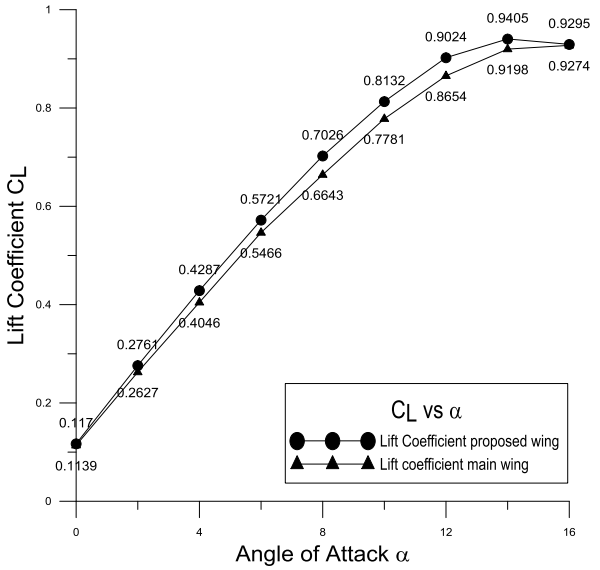

Figure 19. Lift coefficient C_L vs α .

Table 2. Drag coefficient C_D vs α.

Air Velocity V∞ (m/s)	α	C_D Proposed Wing	C_D Main Wing
50	0	0.020441	0.021204
	2	0.025097	0.025621
	4	0.033221	0.033632
	6	0.046017	0.047142
	8	0.066976	0.067612
	10	0.093391	0.093706
	12	0.125221	0.125686
	14	0.162042	0.162649
	16	0.193253	0.200721

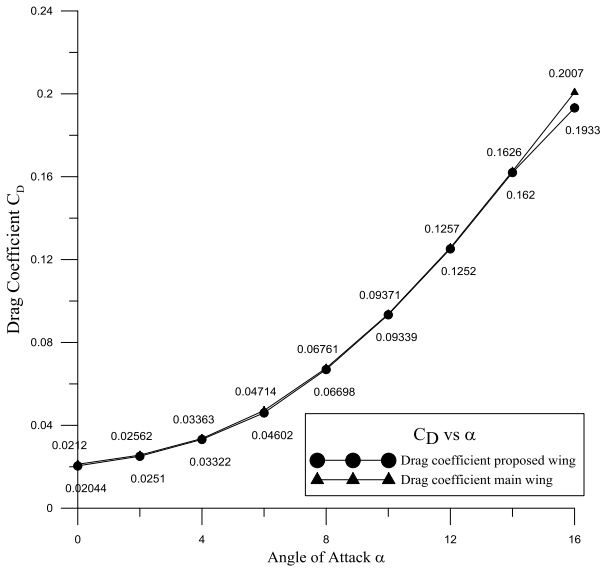

Figure 20. Drag coefficient C_D vs α.

Table 3. C_L/C_D ratio vs α.

Air Velocity V∞ (m/s)	α	CL/CD Proposed Wing	CL/CD Main Wing
50	0	5.724969	5.370089
	2	11.00307	10.25464
	4	12.90501	12.03141
	6	12.43239	11.59456
	8	10.48986	9.82553
	10	8.707594	8.303718
	12	7.206637	6.885478
	14	5.803775	5.655348
	16	4.809647	4.620469

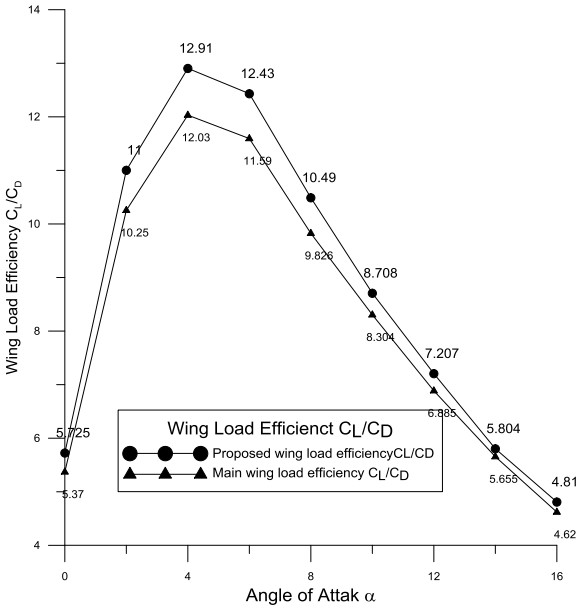

Figure 21. CL/CD ratio vs α.

Table 4. C_D/C_L Ratio vs α.

Air Velocity V∞ (m/s)	α	C_D/C_L Proposed Wing	C_D/C_L Main Wing
50	0	0.174673	0.186217
	2	0.090884	0.097517
	4	0.077489	0.083116
	6	0.080435	0.086247
	8	0.09533	0.101776
	10	0.114842	0.120428
	12	0.138761	0.145233
	14	0.172302	0.176824
	16	0.207915	0.216428

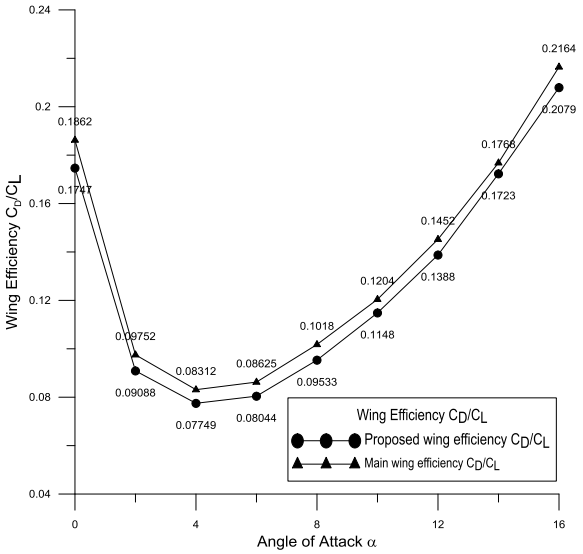

Figure 22: C_D/C_L Ratio vs α.

Table 5. Induct drag C_{Di} vs α.

Air Velocity V∞ (m/s)	α	C_{Di} Proposed Wing	C_{Di} Main Wing
50	0	0.000764	0.00088
	2	0.004255	0.004682
	4	0.010256	0.011107
	6	0.018264	0.020266
	8	0.027544	0.029936
	10	0.036903	0.041069
	12	0.045444	0.050801
	14	0.049355	0.057393
	16	0.048209	0.058343

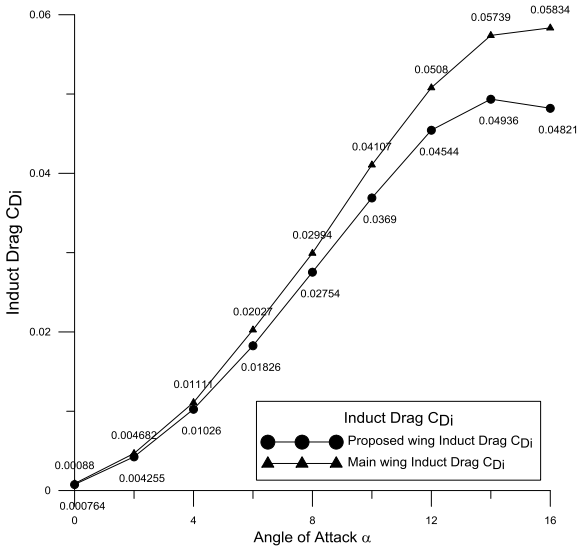

Figure 23. Induct drag C_{Di} vs α.

Table 6. Lift force L vs α.

Air Velocity V∞ (m/s)	α	L Proposed Wing	L Main Wing
50	0	2329.489	2196.953
	2	5496.937	5069.052
	4	8534.152	7807.089
	6	11388.47	10545.9
	8	13985.55	12817.34
	10	16187.98	15012.61
	12	17963.9	16696.9
	14	18720.95	17747.11
	16	18502.4	17893.47

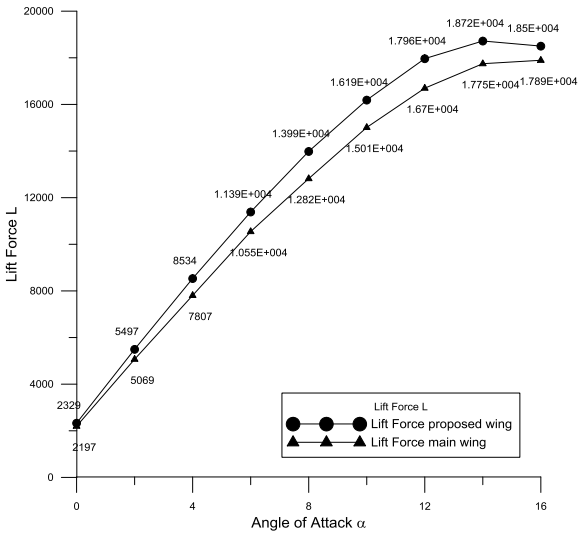

Figure 24. Lift force L vs α.

Table 7: Drag force D vs α.

Air Velocity V∞ (m/s)	α	D Proposed Wing	D Main Wing
50	0	389.6239	406.9037
	2	470.7741	499.5772
	4	617.9864	661.3055
	6	866.2346	916.0318
	8	1242.371	1333.245
	10	1721.846	1859.065
	12	2309.471	2492.689
	14	2988.677	3225.651
	16	3688.204	3846.943

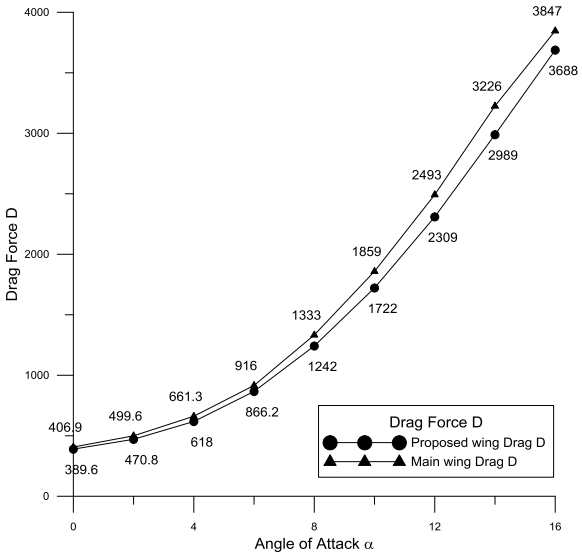

Figure 25. Drag force D vs α.

Table 8. Induct angle of attack (α_i) and effective angle of attack (α_{eff}) vs α.

Air Velocity V∞ (m/s)	α	α_i Proposed Wing	α_{eff} Proposed Wing	α_i Main Wing	α_{eff} Main Wing
50	0	0.005551	-0.00555	0.006565	-0.00657
	2	0.013098	1.986902	0.015148	1.984852
	4	0.020335	3.979665	0.023331	3.976669
	6	0.027136	5.972864	0.031515	5.968485
	8	0.033324	7.966676	0.038303	7.961697
	10	0.038572	9.961428	0.044864	9.955136
	12	0.042804	11.9572	0.049897	11.9501
	14	0.044608	13.95539	0.053035	13.94696
	16	0.044087	15.95591	0.053473	15.94653

Table 9. Improvement of proposed modification wing with raked winglets comparing to the baseline main wing model.

Air Velocity V_∞ (m/s)	α	Gain C_L%	Gain C_D%	Gain C_L/C_D%	Gain C_{Di}%
50	0	2.77%	3.60%	6.61%	13.11%
	2	5.10%	2.04%	7.30%	9.12%
	4	5.95%	1.22%	7.26%	7.65%
	6	4.67%	2.39%	7.23%	9.88%
	8	5.76%	0.94%	6.76%	7.99%
	10	4.51%	0.34%	4.86%	10.14%
	12	4.28%	0.37%	4.66%	10.55%
	14	2.24%	0.37%	2.62%	14.01%
	16	0.22%	3.72%	4.09%	17.37%